X-ray Characterizations of Polyethylene Polyhedral Oligomeric Silsesquioxane Copolymers

Lei Zheng, Alan J. Waddon,* Richard J. Farris, and E. Bryan Coughlin*

Polymer Science and Engineering Department, University of Massachusetts, Amherst, Massachusetts 01003

Received October 24, 2001; Revised Manuscript Received December 10, 2001

ABSTRACT: A novel nanocomposite containing polyethylene and polyhedral oligomeric silsesquioxane (POSS) nanoparticles has been characterized using wide-angle X-ray scattering (WAXS). In copolymers formed between ethylene and POSS containing macromonomers, the POSS units, attached as pendant groups off the polyethylene backbones, are found to aggregate and crystallize as nanocrystals. The POSS nanoparticles in such PE-*co*-POSS copolymers form a lattice separate from the PE lattice with characteristic diffraction signals. From both line broadening of the diffraction maxima and also the oriented diffraction in a drawn material, we conclude that POSS crystallizes as anisotropically shaped crystallites. The presence of POSS disrupts the crystallization of polyethylene and results in less and smaller/disordered polyethylene crystallites. POSS nanocrystals are covalently connected to the PE crystallites via an intermediate disordered interfacial region. The PE crystallites are reinforced by the POSS crystallites, maintaining their crystalline structure under high draw ratio. In total, these contributions help to explain the novel properties of this type of nanocomposite, such as better dimensional stability, extension of high-temperature rubbery plateau, and strong thermal oxidative resistance.

Introduction

Organic−inorganic nanocomposite materials[1−6] have attracted a great deal of attention recently due to their potential as candidate materials for bridging the gap between organic polymers and inorganic ceramics. In particular, the use of polyhedral oligomeric silsesquioxane (POSS)[7] nanoparticles has been demonstrated to be an efficient method in the design of hydrid materials.[5,6,8−18] A typical POSS macromonomer has an inorganic Si_8O_{12} core surrounded by seven organic groups (e.g., cyclopentyl or cycylohexyl) on the corners, which promote solubility in conventional solvents, and one unique group at the final corner which is used as the site of polymerization with an assorted array of comonomers (Figure 1). Copolymers obtained in this manner include copolymers of polysiloxane,[8,15] poly(methyl methacrylate),[9] poly(4-methylstyrene),[10,12] epoxy,[11,13] polynorbornene,[14] and polyurethane.[17,18] They represent a new category of polymers characterized by the presence of bulky POSS nanoparticles.

In general, POSS containing copolymers have higher mechanical and thermal properties than the polymers without POSS side units. However, neither the microstructure of this category of polymers nor the mechanism of reinforcement is well understood. Such reinforcement may, in principle, arise either from isolated POSS nanoparticle units or from aggregates of these units into larger POSS clusters. The degree of aggregation may be expected to depend on the mole fraction of POSS nanoparticles, the lattice energy of POSS crystals, the degree of compatibility of the POSS with the host polymer component, and the tendency for this host component to form a separate crystalline phase. There are literature reports ascribing mechanical reinforcement to both isolated POSS nanoparticles and POSS aggregates. For example, the increase and broadening of glass transition temperature with increasing POSS loadings in a POSS epoxy cross-linked system was attributed to the nanoscopic size of individual POSS nanoparticles which hindered the motion of molecular chain network junctions.[11] Rheological measurements on amorphous linear poly(4-methylstyrene)-*co*-POSS copolymers found a high-temperature rubbery plateau, suggesting that associative interactions between POSS nanoparticles were responsible for retarding polymer chain motion.[12] Mechanical relaxation measurements and WAXS of amorphous polynorbornene-*co*-POSS copolymers with different pendant R groups on POSS nanoparticles indicated that ordering in POSS aggregates at the nanometer scale was better in cyclopentyl-substituted POSS than cyclohexyl-substituted POSS.[14] On the other hand, a report based on atomistic molecular dynamics simulation of the same system concluded that aggregation of the POSS nanoparticles was not required for reinforcement effects, such as the increase in glass transition temperature and retardation of chain dynamics. The lack of mobility of individual POSS nanoparticles, with an approximate spherical diameter of 1.5 nm (comparable to that of polymer segments), was reasoned to be the primary source for the beneficial effects.[19] Conceptionally, the reinforcement of a copolymer by aggregates of POSS should be distinguished

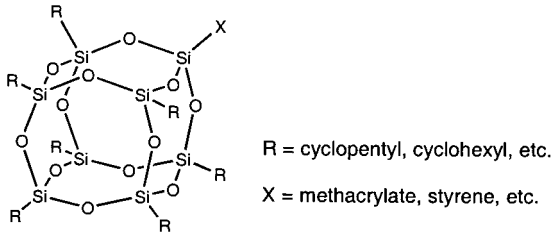

Figure 1. POSS macromonomer structure.

* To whom correspondence should be addressed. E-mail: E. B. Coughlin coughlin@mail.pse.umass.edu; A. J. Waddon waddon@polysci.umass.edu.

10.1021/ma011855e CCC: $22.00
Published on Web 02/13/2002

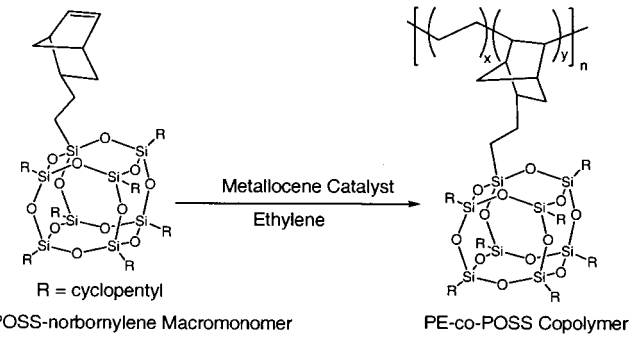

Figure 2. Synthesis of PE-*co*-POSS copolymers.

Table 1. Molecular Characterization of PE-*co*-POSS Copolymers

sample	POSS in copolymers (wt %)	POSS in copolymers (mol %)	M_w ($\times 10^3$ g/mol)	PDI
PE	0	0	328	1.26
PE−POSS1	19	0.64	315	1.43
PE−POSS2	27	1.0	315	1.67
PE−POSS3	37	1.6	516	1.73
PE−POSS4	56	3.4	446	2.07

from any reinforcement caused simply by the bulky nature of individual POSS nanoparticles in cases where the POSS units do not crystallize.

A body of work has shown that octasubstituted alkyl-substituted POSS nanoparticles $R_8Si_8O_{12}$ with various R groups (R = hydrogen, methyl, ethyl, isopropyl, cyclohexyl, or phenyl) form rhombohedral (hexagonal) crystal structures with similar WAXS "fingerprints".[20−24] POSS nanoparticles can also form crystalline aggregates when attached as pendant groups to a host chain by copolymerization. This occurs with a variety of copolymers ranging from random to block.[12,14,25] The POSS component in all these copolymers showed similarities in their X-ray diffraction patterns. Moreover, these patterns were similar to those from crystals of unattached POSS nanoparticles (described above), suggesting that, in POSS containing copolymers, POSS aggregates may also crystallize in a similar rhombohedral geometry. However, detailed study is needed to fully determine the structures.

Most previous work, with some exceptions,[18] has focused on amorphous host polymers which are inherently uncrystallizable. The present work now extends this to a fundamentally different class of materials in which the host polymer is itself highly crystallizable in the homopolymer state. In the copolymers there is, of course, a strong tendency for ordered aggregation and crystallization of the host polymer segment, which therefore competes with POSS aggregation and crystallization. Recently, we reported a novel class of copolymers of this type. These polyethylene-*co*-POSS (PE−POSS) copolymers with bulky POSS nanoparticles covalently attached to the polyethylene backbone were synthesized using metallocene-catalyzed polymerization (Figure 2).[26] These polymers displayed enhanced thermal properties and dimensional stability. The microstructure of this new class of materials is undetermined and presents an interesting and also practically important problem. This work addresses this issue.

Experimental Section

Polymer samples were synthesized according to our previous report.[26] The precipitated polymers were pressed into films on a Carver press at 180 °C for 10 min between two Kapton films. They were then cooled to room temperature by circulating water through the hot plates. The transparent films were roughly 0.2 mm thick. The POSS content varied from 19 wt % (0.64 mol %) to 56 wt % (3.4 mol %) (Table 1). Attention is drawn to the fact that, at even very small mole fractions, the weight fraction of POSS is substantial. An example material (37 wt %, 1.6 mol %) was oriented by drawing in the solid state at 90 °C to a draw ratio of ~3 using an Instron 5564 equipped with an environmental chamber.

WAXS images were obtained using an evacuated Statton camera with a 10 cm × 15 cm Fuji image plate. Cu Kα radiation (wavelength 1.54 Å) was used with a nickel filter. The X-rays were collimated into a fine beam of circular cross section using a pinhole collimator. Calcite was used to calibrate the camera length. The scattering patterns were scanned on a Fuji BAS-2500 image plate scanner. Intensity profiles were obtained from radial averages of the scattering pattern intensities. The drawn film was examined with the beam both normal and edge-on to the plane of the film.

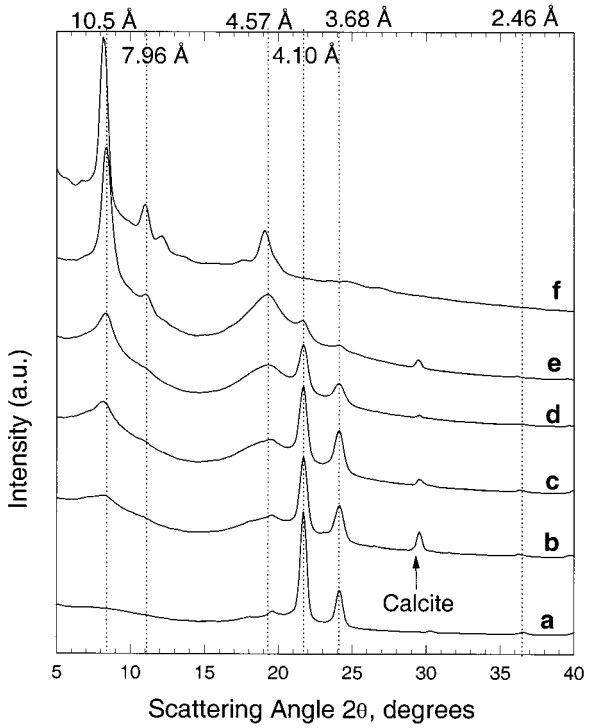

Figure 3. Line profiles of WAXS data of PE-*co*-POSS copolymers: (a) PE, (b) PE−POSS 19 wt % (0.64 mol %), (c) PE−POSS 27 wt % (1.0 mol %), (d) PE−POSS 37 wt % (1.6 mol %), (e) PE−POSS 56 wt % (3.4 mol %), (f) POSS−norbornylene macromonomer.

Results

The X-ray scattering profiles of PE−POSS1−4 are shown in Figure 3b−e. For comparison, traces of homopolyethylene and the POSS macromonomer are also shown, a and f, respectively. The pure PE shows reflections at 2θ's of 21.4° (4.10 Å), 24.2° (3.68 Å), and 36.5° (2.46 Å), corresponding to the 110, 200, and 020 reflections of the usual orthorhombic PE crystal structure. A weaker reflection at $2\theta = 19.6°$ (4.52 Å) is the 010 reflection from the commonly observed but minor component of the monoclinic crystal structure of PE. The pure POSS macromonomer shows strong reflections at 2θ's of 8.2° (10.8 Å), 11.0° (8.03 Å), and 19.0° (4.66 Å).

It is clear that the copolymers show crystalline features that are characteristic of the structures of the two separate components. The PE-*co*-POSS sample with lowest POSS content in this series is dominated by the

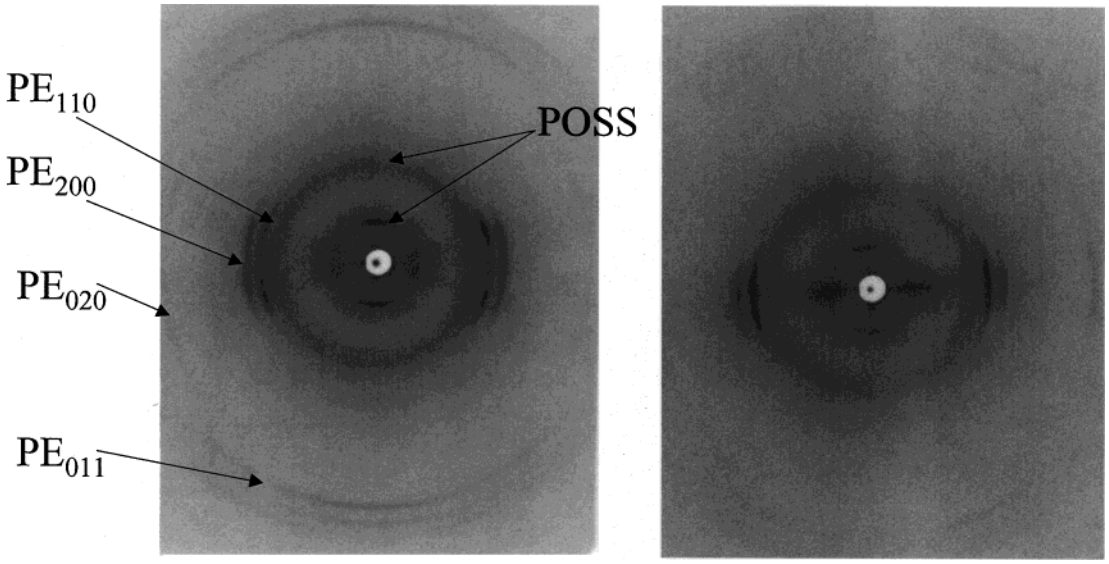

Figure 4. WAXS pattern of PE−POSS 37 wt % copolymer (drawing direction is vertical, 3×): (a) X-ray beam was normal to the film, (b) X-ray beam was edge-on to the film.

PE crystal component. However, two additional broad peaks at 8.4° (10.5 Å) and 19.4° (4.57 Å) also appear. These clearly correspond to the strongest of the POSS reflections (trace f). As the POSS content increases, the reflections from the POSS component increase in intensity and sharpness, while the PE reflections weaken and broaden. At the highest POSS content, 56 wt % (3.4 mol %), the sample shows only weak PE crystal peaks, leading to the conclusion that the PE component (which forms ∼44 wt % and 97 mol % of the material) must be primarily disordered. It is also notable that, with progressive increase in POSS content, although the PE crystallinity is much lower, where there are PE crystals, the PE peak positions remain constant, therefore indicating that the crystal lattice is not expanded.

The progressive intensification and sharpening of the POSS reflections clearly show the progressive development of a distinct ordered POSS lattice at the expense of the crystallinity of PE. Simple estimation of the apparent crystallite size dimensions (L), based on the half-widths of reflections (β) at 10.5 Å using Scherrer's equation ($L = \lambda/(\beta \cos \theta)$), indicates a gradual increase in the POSS crystallite size and/or order with POSS content (PE−POSS1 ∼40 Å to PE−POSS4 ∼100 Å). We especially draw attention to the difference in line broadening between the POSS peaks at 4.57 and 10.5 Å. The difference in the width of the 10.5 Å peak compared with that at 4.57 Å is far greater in the copolymers than in the macromonomer, indicating an anisotropy in apparent crystallite size in the copolymers which is not displayed in the POSS macromonomer (Figure 3).

The diffraction pattern of the film drawn at 90 °C is shown in Figure 4. With the beam normal to the sample plane two crystalline components, originating from the PE and the POSS, can again be identified. Both PE_{110} and PE_{020} appear as two arcs above and below the equator (plus or minus ∼16°). The large apparent equatorial spread of PE_{200} is also considered to be due to separation into two reflections above and below the equator. The near meridional reflection (at 2.23 Å) is identified as PE_{011}. Turning to the POSS component, the POSS reflection at 10.5 Å appears meridionally, while the broad POSS reflection at 4.57 Å forms a continuous ring. With the beam edge-on, the POSS 10.5 Å reflection is again meridional, while both PE_{110} and PE_{200} are equatorial.

Discussion

Most previous work on polymeric materials containing POSS nanoparticles included as pendant groups has concerned host polymers which are themselves inherently uncrystallizable. In such copolymers, aggregation and crystallization of POSS are limited primarily by the topology of the host chain. Our system of PE−POSS is distinct from these other systems in that crystallization of both POSS and PE chain segments may occur, and the final microstructure may be controlled not only by host chain topology but also by the competition between the two crystallization processes. In these PE−POSS copolymers the PE crystallinity and apparent crystal sizes become progressively smaller with increasing POSS concentration. This is presumably because POSS nanoparticles disrupt the crystallization of polyethylene crystals by virtue of their size (∼1.5 nm for each POSS group). It is clearly impossible for such large units to be accommodated within the PE crystal structure, and, in this respect, it is noted that the PE lattice parameters appear to be essentially unchanged over the entire range of loading. Nevertheless, the crystallization of PE is evidently limited by the presence of POSS groups along the chain even at low POSS mole fractions.

With increasing POSS mole fraction, it is also seen that the amount of POSS crystallization increases. The *d*-spacing values for our POSS nanocrystals (10.5, 7.96, and 4.57 Å) are very similar to those reported in other polymer systems containing POSS nanoparticles, such as the homopolymer of POSS−styryl[12] and the block copolymer of poly(methyl acrylate)-*block*-POSS.[25] In these reports, the most intense reflection was at a spacing of approximately 10−11 Å, and this sharpened with increasing POSS concentration. However, the peak at 4−5 Å seemed relatively broad and diffuse. Despite the different polymer host, it is reasonable to conclude that the POSS crystallites in all these copolymers have similar packing structures or unit cells. Moreover, the patterns from the copolymers are very similar to those from the POSS macromonomer, leading us to conclude

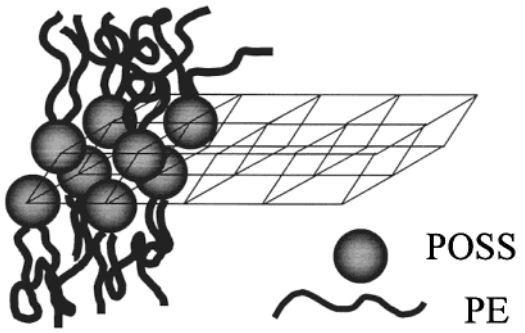

Figure 5. Schematic drawing of a two-dimensional POSS lattice formed in PE−POSS copolymers.

that the packing in the copolymers is very similar to the rhombohedral (hexagonal) packing of the POSS macromonomer crystal in the absence of a host polymer. Such differences as there are between POSS structures in different host systems may reasonably be explained by differences in spatial and topological constraints.

Consideration of the crystallization of large units of POSS, which are attached as side groups to a polymer chain, quickly leads to the realization that there are considerable spatial constraints imposed on the crystal shape. In particular, it becomes clear that development in three-dimensions is impossible and that crystals will necessarily form either a columnar (1-dimensional) nanocrystal, with the polymer chain decorating the outside of the crystal, or, at best, a lamellar (2-dimensional) nanocrystal, again with the polymer lying on the external faces of the lamellae (Figure 5). This, of course, is entirely consistent with the preferential broadening of selected WAXS signals with others remaining noticeably sharper. Specifically, the signals at 4.57 and 10.5 Å in the copolymers can therefore be associated with planes approximately perpendicular to the short and long dimensions of the nanocrystal, respectively.

The distance between two POSS particles in the lattice of the copolymers is slightly smaller than that of the macromonomer on the basis of diffraction peak positions (i.e., larger 2θ) (8.4° vs 8.2°, 11.1° vs 11.0°, and 19.4° vs 19.0°; Figure 3, e vs f). Again, this can be explained by our proposed constrained lattice in copolymers. In a three-dimensional lattice of POSS particles the lattice accommodates the substituted norbornylene group, which is slightly larger than the cyclopentyl groups on the remaining corners; in a dimensionally constrained crystal of POSS copolymers the large norbornylene groups, which are connected to the polymer backbones, are likely to be excluded from the lattice (Figures 2 and 5).

Further information is obtained from the oriented WAXS from the drawn material (Figure 4). The texture is consistent with the 10.5 Å spacing in the POSS crystal (considered to be the long axis in the crystallites) lying parallel to the draw direction. The PE WAXS component does not show simple chain orientation; rather, this appears consistent with a texture with $\mathbf{c}_{PE}$ lying in the plane of the film but inclined at a slight angle to the draw direction and in which $\mathbf{a}_{PE}$ and $\mathbf{b}_{PE}$ are randomized about c_{PE}. Therefore, $hk0$'s appear equatorial in the edge-on projection in WAXS (Figure 4b), and the inclination of $\mathbf{c}_{PE}$ to the draw direction is only revealed in the normal projection (Figure 4a). Moreover, the angle of inclination of $\mathbf{c}_{PE}$ was found to be variable. Clearly, as opposed to orientation of chains, drawing has rather promoted orientation of the crystallites. It is important to note that drawing was carried out below the melting point of both crystal components. The oriented pattern indicates that POSS crystallites have aligned parallel to the drawing direction while the PE crystals are inclined at some variable angle to this direction. The variability of the alignment of PE crystallites with respect to the draw direction (and therefore to the alignment of the POSS crystals) suggests that the two crystalline components are not directly in contact and that they must be separated by a region of uncrystallized material (hence providing a location for the considerable quantity of uncrystallized PE). The POSS crystallites are clearly the features primarily aligning along the draw direction, and these, in turn, "pull" and "rotate" the PE crystallites with them. The absence of chain orientation, even at a relatively high draw ratio of ∼3, may also be explained by the covalent connectivity between the PE and POSS. Such chain orientation would require the PE crystallites to "pull out" and fragment and, accordingly, would also require the POSS crystallites to fragment. The POSS crystals can then be regarded as a source of reinforcement for the PE crystallites.

This, of course, has implications for other properties. The observed improvement of dimensional stability, with retention of shape well above the melting temperature of polyethylene, can also be attributed to POSS nanocrystals acting as physical cross-linking points. The observed extension of the rubbery plateau above the melting temperature of polyethylene in mechanical tests is also explicable in these terms.[26] Such a POSS structure may also be expected to play a role in the improved oxidative stability seen in PE−POSS nanocomposites, facilitating the formation of an effective protective coating of SiO_2.[27] Indeed, the formation of POSS nanocrystals readily explains the change in rheological properties and the increase of glass transition temperature observed in many other POSS copolymers.

Finally, the interfacial property of POSS nanoparticles can be tuned by changing the substitution groups R at the corners of each POSS unit (Figure 1), to increase or decrease the compatibility between the POSS and polymer matrix. In our specific system, with cyclopentyl groups on POSS and a PE matrix, we found very clear separation of the two components into different crystal domains.

Conclusion

Polyethylene-*co*-POSS random copolymers of 0.64−3.4 mol % (corresponding to 19−56 wt %) have been characterized using WAXS. Crystallites of both polyethylene and pendant POSS nanoparticles were found to coexist in the copolymers. This leads to a "mutually dependent" microstructure in which no one component can be said to be controlling. The presence of POSS nanoparticles lowers the crystallinity of the PE component and results in smaller/disordered PE crystallites. On the other hand, POSS crystallites do not show full three-dimensional development but rather grow within spatial constraints imposed by the presence of the polymer chain, leading to an anisotropic crystallite shape. The anisotropic shape of the POSS crystallites was particularly displayed during mechanical drawing at elevated temperature (but below the melting point). The anisotropic POSS crystallites were found to be the

primary component responding to the draw, aligning with their major dimension parallel to the draw direction. The PE crystallites (of course, covalently attached to the POSS crystallites) were less responsive to the draw. This leads us to conclude that the surfaces of the PE and POSS crystals cannot be connected directly and that disordered material must lie within this interfacial region.

The POSS lattice formed shows very similar diffraction characteristics both to crystals of unpolymerized POSS macromonomer and to those reported in POSS crystals formed in other POSS containing copolymers. Consequently, it was concluded that very similar crystal structures were formed in all these cases.

An important conclusion from this study is that an anisotropically shaped, inorganic structure is formed from isotropic POSS nanoparticles covalently bonded to polymer chains (which are the source of the limitation of POSS crystal growth). The use of POSS as assembling blocks of aggregated structures may open the door for the design and synthesis of novel type of nanocomposites. Many physical properties observed in clay polymer nanocomposites, such as low gas permeability, can also be envisaged in polymer systems containing anisotropic nanostructures of POSS.

Acknowledgment. Financial support was provided by the NSF sponsored Materials Research Science and Engineering Center (MRSEC) at University of Massachusetts and 3M (for a faculty award to E. B. Coughlin).

References and Notes

(1) Pinnavaia, T. J., Beal, G. W., Eds. *Polymer Clay Nanocomposites*; John Wiley & Sons: New York, 2001.
(2) Giannelis, E. P. *Adv. Mater.* **1996**, *8*, 29−35.
(3) Kojima, Y.; Usuki, A.; Kawasumi, M.; Okada, A.; Kurauchi, T.; Kamigaito, O. *J. Polym. Sci., Part A: Polym. Chem.* **1993**, *31*, 983−986.
(4) Sellinger, A.; Weiss, P. M.; Nguyen, A.; Lu, Y. F.; Assink, R. A.; Gong, W. L.; Brinker, C. J. *Nature (London)* **1998**, *394*, 256−260.
(5) Lichtenhan, J. D. In *Polymeric Materials Encyclopedia*; Salamone, J. C., Ed.; CRC Press: Boca Raton, FL, 1996; pp 7768−7777.
(6) Schwab, J. J.; Lichtenhan, J. D. *Appl. Organomet. Chem.* **1998**, *12*, 707−713.
(7) POSS is a trademark of Hybrid Plastics (www.hybridplastics.com).
(8) Lichtenhan, J. D.; Vu, N. Q.; Carter, J. A.; Gilman, J. W.; Feher, F. J. *Macromolecules* **1993**, *26*, 2141−2142.
(9) Lichtenhan, J. D.; Otonari, Y. A.; Carr, M. J. *Macromolecules* **1995**, *28*, 8435−8437.
(10) Haddad, T. S.; Lichtenhan, J. D. *Macromolecules* **1996**, *29*, 7302−7304.
(11) Lee, A.; Lichtenhan, J. D. *Macromolecules* **1998**, *31*, 4970−4974.
(12) Romo-Uribe, A.; Mather, P. T.; Haddad, T. S.; Lichtenhan, J. D. *J. Polym. Sci., Part B: Polym. Phys.* **1998**, *36*, 1857−1872.
(13) Lee, A.; Lichtenhan, J. D. *J. Appl. Polym. Sci.* **1999**, *73*, 1993−2001.
(14) Mather, P. T.; Jeon, H. G.; Romo-Uribe, A.; Haddad, T. S.; Lichtenhan, J. D. *Macromolecules* **1999**, *32*, 1194−1203.
(15) Shockey, E. G.; Bolf, A. G.; Jones, P. F.; Schwab, J. J.; Chaffee, K. P.; Haddad, T. S.; Lichtenhan, J. D. *Appl. Organomet. Chem.* **1999**, *13*, 311−327.
(16) Fu, B. X.; Zhang, W. H.; Hsiao, B. S.; Rafailovich, M.; Sokolov, J.; Johansson, G.; Sauer, B. B.; Phillips, S.; Balnski, R. *High Perform. Polym.* **2000**, *12*, 565−571.
(17) Hsiao, B. S.; White, H.; Rafailovich, M.; Mather, P. T.; Jeon, H. G.; Phillips, S.; Lichtenhan, J.; Schwab, J. *Polymer* **2000**, *49*, 437−440.
(18) Fu, B. X.; Hsiao, B. S.; Pagola, S.; Stephens, P.; White, H.; Rafailovich, M.; Sokolov, J.; Mather, P. T.; Jeon, H. G.; Phillips, S.; Lichtenhan, J.; Schwab, J. *Polymer* **2001**, *42*, 599−611.
(19) Bharadwaj, R. K.; Berry, R. J.; Farmer, B. L. *Polymer* **2000**, *41*, 7209−7221.
(20) Barry, A. J.; Daudt, W. H.; Domicone, J. J.; Gilkey, J. W. *J. Am. Chem. Soc.* **1955**, *77*, 4248−4252.
(21) Larsson, K. *Ark. Kemi* **1960**, *16*, 203−228.
(22) Larsson, K. *Ark. Kemi* **1960**, *16*, 209−214.
(23) Larsson, K. *Ark. Kemi* **1960**, *16*, 215−219.
(24) Auf der Heyde, T. P. E.; Burgi, H.-B.; Burgy, H.; Tornroos, K. W. *Chimia* **1991**, *45*, 38−40.
(25) Mather, P. T.; Chun, S. B.; Pyun, J.; Matyjaszewski, K. *Polym. Prepr. (Am. Chem. Soc.)* **2000**, *41* (1), 582.
(26) Zheng, L.; Farris, R. J.; Coughlin, E. B. *Macromolecules* **2001**, *34*, 8034−8039.
(27) Gonzalez, R. I.; Phillips, S. H.; Hoflund, G. B. *J. Spacecr. Rockets* **2000**, *37*, 463−467.

MA011855E